Transient 2D-IR Spectroscopy: Snapshots of the Nonequilibrium Ensemble during the Picosecond Conformational Transition of a Small Peptide

Jens Bredenbeck,[†] Jan Helbing,[†] Raymond Behrendt,[‡] Christian Renner,[‡] Luis Moroder,[‡] Josef Wachtveitl,[§] and Peter Hamm*,[†]

Universität Zürich, Physikalisch Chemisches Institut, Winterthurer Strasse 190, CH-8057 Zürich, Switzerland, Max-Planck-Institut für Biochemie, Am Klopferspitz 18A, D-82152 Martinsried, Germany, and Johann Wolfgang Goethe Universität Frankfurt am Main, Institut für Physikalische und Theoretische Chemie, Marie-Curie-Strasse 11, D-60439 Frankfurt am Main, Germany

Received: March 4, 2003; In Final Form: June 4, 2003

The technique of transient two-dimensional infrared (T2D-IR) spectroscopy is introduced, which extends the advantage of 2D-IR spectroscopy to the investigation of a transient species with picosecond time resolution. The conformational change of a small cyclic peptide is studied in the amide-I spectral range, which is induced by means of a photoswitch integrated into the peptide backbone. Substantial changes are found in the transient 2D-IR spectra at times when the transient 1D spectra show only a minor time dependence, illustrating the information gain accessible from 2D-IR spectroscopy. In contrast to 1D spectroscopy, 2D-IR can distinguish between homogeneous and inhomogeneous broadening. The homogeneous contribution to the total width of the amide-I band changes during the course of the conformational transition, a result that is interpreted in terms of the manner in which the peptide samples its conformational space.

I. Introduction

Recent work has shown that nonlinear 2D infrared (2D-IR) spectroscopy might be a valuable experimental complement to 2D-NMR for studying molecular systems.[1−14] Two-dimensional IR spectroscopy yields much more detailed information on the vibrational Hamiltonian of a molecular system than one-dimensional IR spectroscopy. In the case of small peptides, 2D-IR spectroscopy allows one to measure the coupling between certain vibrational modes of different peptide units within the polypeptide chain. The vibrational modes under study are the so-called amide-I modes (mostly a C═O stretching vibration of the peptide unit) located between 1600 and 1700 cm^{-1}. Because the coupling strength is related to the relative orientation of the peptide units,[15−17] one can obtain structural information from a 2D-IR spectrum. This has been demonstrated recently in the case of Ala-Ala-Ala (trialanine),[13,14] the smallest conceivable system with only two peptide units. Subpicosecond equilibrium fluctuations of the peptide backbone around its preferred conformation have been addressed as well by investigating the population transfer between both peptide units.[18] Furthermore, the width of the structural distribution of trialanine has been analyzed by exploring the inhomogeneity of the 2D-IR spectra.[19]

The most promising potential of 2D-IR spectroscopy is its intrinsic high time resolution of about 1 ps—many orders of magnitude faster than what 2D-NMR spectroscopy can achieve—which allows for freezing in all but the fastest subpicosecond motions of the peptide backbone. Until now, 2D-IR spectroscopy has been applied only to equilibrium states, in which case the high time resolution helps to distinguish between dynamically coupled subconformations.[19] This work reports on our first efforts in performing *transient* 2D-IR (T2D-IR) spectroscopy of a nonequilibrium ensemble, in which case the high time resolution can be taken full advantage of.

The molecule chosen for this study is a bicyclic octapeptide (bcAMPB) containing a photoresponsive azobenzene moiety.[20] The azobenzene unit can be reversibly switched between the cis and trans conformations using light of different wavelengths, thereby predetermining the conformation of the peptide backbone. According to NMR investigations,[20] the cis state is a frustrated system with many close-lying conformational energy minima, but the backbone structure of the trans conformation is much more stretched as a result of the larger end-to-end distance of the azobenzene unit. The cis → trans isomerization of the azobenzene unit itself is completed within less than a picosecond with a quantum efficiency of ∼50%.[21] The time scales of the response of the peptide backbone on the changed restraint have been investigated in detail in recent work,[22] where we employed conventional UV pump−IR probe spectroscopy (transient 1D-IR spectroscopy, T1D-IR) of the amide-I band. Two major phases have been observed during the conformational transition: During a fast-driven phase, the peptide backbone is forced into a stretched conformation by the isomerizing azobenzene unit. The stretching is essentially finished after a surprisingly short time of 20 ps and can be imagined to be a downhill process on a steep part of the potential energy surface of the peptide. The stretched system is still not at equilibrium and subsequently relaxes on a discrete hierarchy of time scales that continues for longer than 16 ns. In the present work, we present transient 2D-IR (T2D-IR) snapshots of the peptide ensemble taken during the transition from the cis to the trans configuration.

II. Principles of Transient 2D-IR Spectroscopy

The 2D-IR part of the experiment is performed according to our previously described double-resonance scheme:[3,5] The center frequency ω_{pu} of a spectrally tunable, narrow-band IR

* Corresponding author. E-mail: phamm@pci.unizh.ch.
[†] Universität Zürich.
[‡] Max-Planck-Institut für Biochemie.
[§] Johann Wolfgang Goethe Universität Frankfurt am Main.

10.1021/jp034552q CCC: $25.00
Published on Web 07/15/2003

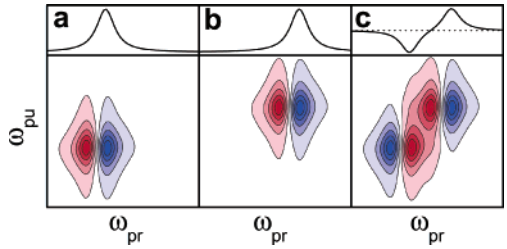

Figure 1. Schematic illustration of transient 1D (top) and 2D-IR (bottom) spectroscopy. The absorption frequency shifts from steady state a to b, each yielding a characteristic 2D-IR spectrum. In c, difference 1D and 2D-IR spectra are shown. The negative response is depicted in blue, and the positive response, in red.

pump pulse is tuned across the amide-I band to construct 2D-IR spectra as a function of the IR pump and IR probe frequencies ω_{pu} and ω_{pr}, respectively. By the addition of an UV pulse preceding the 2D-IR part of the experiment, the 2D-IR spectrum of the photoswitched ensemble is recorded. Hence, the total experiment consists of three pulses: an UV pump, a narrow-band IR pump, and a broad-band IR probe pulse. Because we cannot convert 100% of the initial species into the product species, the 2D-IR spectrum in the presence of the UV switch pulse always contains contributions from both. To eliminate contributions of molecules that have not absorbed an UV photon, two sets of 2D-IR spectra are recorded simultaneously—one with the UV switch pulse on and one with the UV switch pulse off—and subtracted from each other. Hence, as is common practice in conventional pump−probe spectroscopy, our T2D-IR spectra are in fact T2D-IR *difference* spectra.

To facilitate the discussion, we introduce a schematic T2D-IR spectrum of an idealized molecule with a single homogeneously broadened oscillator, the frequency of which shifts upon triggering the photoreaction. In both the initial and product states, the vibrator would give rise to a 2D-IR spectrum (Figure 1a and b) given by

$$\Delta A_{2D}(\omega_{pu}, \omega_{pr}) = n_{ex}(\omega_{pu}, \omega_0) \times [A_{hom}(\omega_{pr} - \omega_0 + \delta) - A_{hom}(\omega_{pr} - \omega_0)] \quad (1)$$

where the probability $n_{ex}(\omega_{pu}, \omega_0)$ of exciting the oscillator with the IR pump pulse is a convolution of the pump-pulse spectrum I_{pu} with center frequency ω_{pu} and absorption band A with center frequency ω_0:[3]

$$n_{ex}(\omega_{pu}, \omega_0) = \int_{-\infty}^{\infty} I_{pu}(\omega - \omega_{pu})\, A_{hom}(\omega - \omega_0)\, d\omega \quad (2)$$

Two peaks would be observed in each 2D-IR spectrum: a negative (blue) bleach and stimulated emission signal at the vibrator's original frequency ω_0 and a positive (red) excited-state absorption signal, which is slightly red-shifted owing to the intrinsic anharmonicity δ of the oscillator. The T2D-IR spectrum (Figure 1c) is the difference in the 2D-IR spectra of the initial (Figure 1a) and the transient species (Figure 1b). In a transient 1D difference spectrum, negative contributions arise from the depleted initial population, and positive contributions stem from the transient photoproduct (Figure 1c, top). Accordingly, the signs of the various 2D-IR peaks (color coded in Figure 1) of the initial and product state are also interchanged in the T2D-IR difference spectrum (Figure 1c, bottom). Figure 1c will be used as a guide line to discuss the experimental result. We shall see, however, that the simplistic picture in Figure 1 is not sufficient to account for the dynamic features observed in T2D-IR spectroscopy.

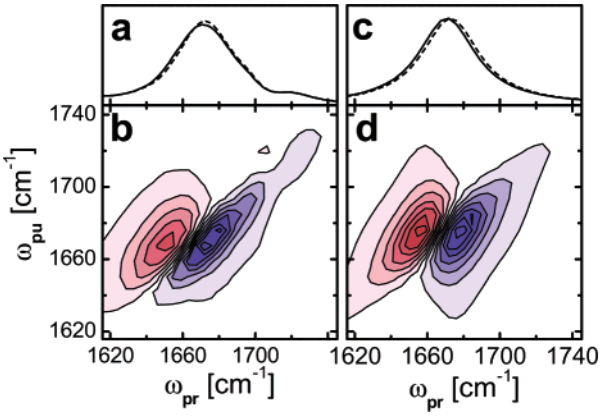

Figure 2. (a) Stationary FTIR spectra of the cis (—) and trans (- - -) states of the cyclic peptide. (b) Stationary 2D-IR spectrum of the cis state for parallel polarization of the pump and probe beams. (c and d) Corresponding spectra from the model calculation. The negative response is depicted in blue, and the positive response, in red.

III. Materials and Methods

The peptide sample (Ala-Cys-Ala-Thr-Cys-Asp-Gly-Phe cyclized by (4-aminomethyl)-phenylazobenzoic acid and oxidized to contain a Cys-Cys disulfide bond[20]) was dissolved in anhydrous dimethyl sulfoxide (DMSO) at a concentration of ~12 mM (absorbance of the amide-I band ~0.3 OD) and circulated through a closed-cycle flow cell designed for small amounts of liquid.[23] Before the experiment was started, the cis−trans equilibrium was shifted to about 80% cis by continuous UV irradiation of the trans $\pi \rightarrow \pi^*$ transition with an Ar ion laser (363 nm, 200 mW). The transition from cis to trans was then initiated by a short 420-nm laser pulse (energy 10 μJ/pulse) obtained from a frequency-doubled 1-kHz Ti:sapphire laser/amplifier system (Spectra-Physics, Spitfire). To allow for a high excitation density (~20%) without inducing nonlinear effects in the sample cell windows (such as white-light generation or color-center formation), the UV pulses were stretched to 700 fs by guiding them through 25 cm of fused silica.

Intense IR pulses (center frequency 1650 cm^{-1}, bandwidth 240 cm^{-1} fwhm, duration 100 fs, energy 1.7 μJ) were generated using a white-light-seeded two-stage BBO optical parametric amplifier, the signal and idler pulses of which were difference-frequency mixed in a $AgGaS_2$ crystal.[24] A small fraction of the IR beam was split off to obtain broad-band probe and reference pulses. The remainder, which was used as the IR pump pulse, was passed through a computer-controlled Fabry−Perot interferometer to generate narrow-band-tunable IR pump pulses (bandwidth ~12 cm^{-1}). The IR pump and probe pulses were focused into the sample in spatial overlap with the 420-nm switch pulse. The reference pulse was focused ~1 mm away. Probe and reference beams were dispersed in a spectrograph and imaged onto a 2 × 32 pixel HgCdTe detector array, which enabled us to measure low-noise (typically 0.003 mOD rms) transient spectra with a spectral resolution of 4 cm^{-1}.

With the help of two light choppers, one in the IR pump beam running at half the repetition rate of the laser system and the other in the UV pump beam running at a quarter of the repetition rate, four individual data sets were recorded: $I_{UV_{on}IR_{on}}$, $I_{UV_{off}IR_{on}}$, $I_{UV_{on}IR_{off}}$, and $I_{UV_{off}IR_{off}}$. The stationary 2D-IR spectrum of the initial state is calculated as (Figure 2b)

$$\Delta A_{2D,stat} = -\log \frac{I_{UV_{off}IR_{on}}}{I_{UV_{off}IR_{off}}} \quad (3)$$

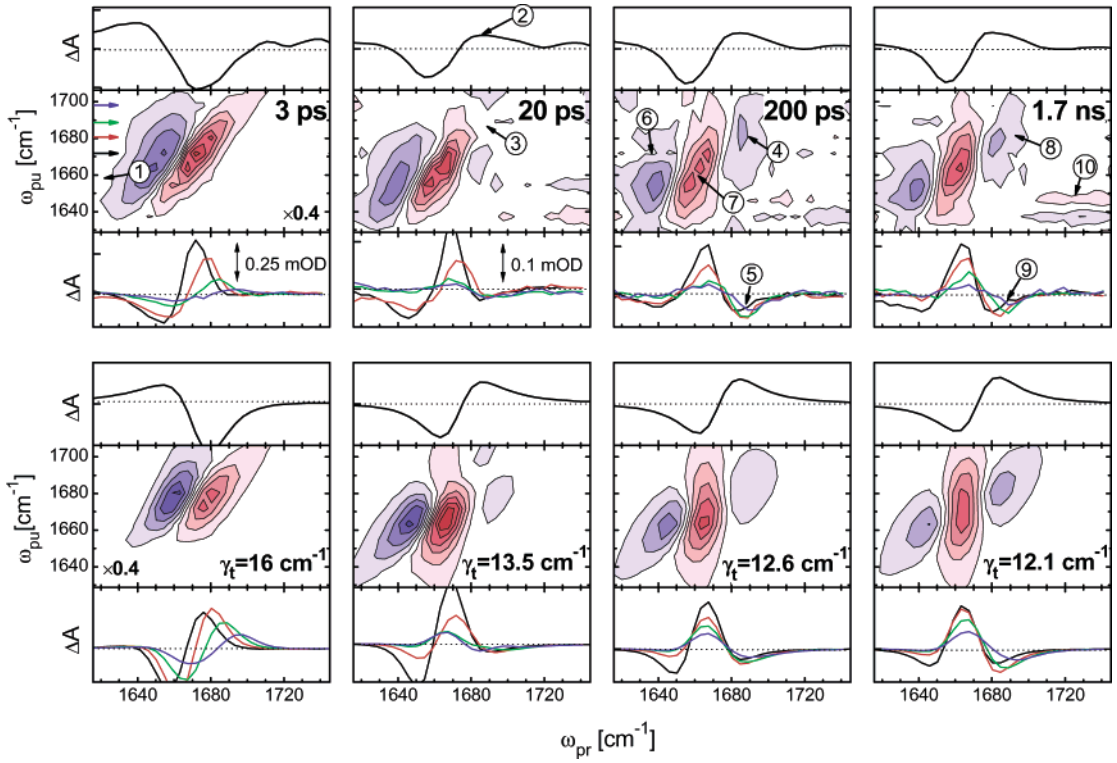

Figure 3. T1D and T2D spectra at UV pump−2D-IR probe delay times of 3 ps, 20 ps, 200 ps, and 1.7 ns. The upper row shows the experimental results, and the lower row, the results of the model calculation. Each panel consists of a T1D spectrum (top) and a T2D spectrum (middle) and cuts through the T2D spectra (bottom) at pump frequencies of 1672 (black), 1689 (red), 1680 (green), and 1689 cm^{-1} (blue, see colored arrows in the 3-ps T2D spectrum). The amplitude of the 3-ps T2D spectrum is larger and has been scaled. All other spectra are on the same linear scale and can be compared directly. In the T2D spectra, negative signals are depicted in blue, and positive signals, in red. The labeled arrows refer to features described in the text.

the T1D-spectra as (Figure 3, top in each panel)

$$\Delta A_{\mathrm{T1D}} = -\log \frac{I_{\mathrm{UV_{on}IR_{off}}}}{I_{\mathrm{UV_{off}IR_{off}}}} \tag{4}$$

and the T2D-IR difference spectra as (Figure 3, middle in each panel)

$$\Delta A_{\mathrm{T2D}} = -\log \frac{I_{\mathrm{UV_{on}IR_{on}}} \cdot I_{\mathrm{UV_{off}IR_{off}}}}{I_{\mathrm{UV_{on}IR_{off}}} \cdot I_{\mathrm{UV_{off}IR_{on}}}} \tag{5}$$

The IR pump−IR probe delay time t_{IR} was fixed at 800 fs (to avoid non-time-ordered pump−probe interactions) in the present study, and the UV pump−2D-IR probe delay time t_{UV} was varied between 3 ps and 1.7 ns. All three pulses were polarized parallel.

IV. Results

Stationary Spectroscopy. The stationary FTIR absorption spectra of the amide-I band of the cis (solid line) and trans (dotted line) species are shown in Figure 2a. They consist of nine amide-I oscillators that are not resolved because of strong broadening mechanisms in the solvent environment. The small wing at $\omega_{\mathrm{pr}} = 1720$ cm^{-1} originates from the carboxyl group in the aspartic acid.

The stationary 2D-IR spectrum of the cis configuration is displayed in Figure 2b. It can be imagined to be a stack of 1D pump−probe spectra recorded for different IR-pump frequencies ω_{pu}. Each pump−probe signal consists of a negative bleach and a stimulated emission (blue) and a positive excited-state absorption (red) contribution, which is slightly red-shifted owing to the intrinsic anharmonicity of the C=O vibrators.[3] When scanning the frequency of the narrow-band pump pulse across the amide-I absorption band, the frequency position of the pump−probe response follows directly. In other words, the narrow-band pump pulse burns holes in the absorption band. The 2D-IR signal is elongated along the diagonal of the 2D-IR spectrum, reflecting the strong inhomogeneity of the amide-I band. This inhomogeneity has to be attributed to two effects: (a) The presence of nine individual amide-I states, which are centered at different frequencies and (b) the spectral inhomogeneity of the individual amide-I vibrators as a result of structural heterogeneity.[19] Cross peaks between the various amide-I states are relatively weak in this type of experiment as a result of the parallel polarization of IR pump and IR probe pulses.[12,10]

Transient 2D-IR Spectroscopy. On the basis of the results of our recent T1D-IR experiments,[22] we have chosen four characteristic delays t_{UV} between the UV switch pulse and the 2D-IR probe: 3 ps, 20 ps, 200 ps, and 1.7 ns. The red shift of the amide-I band at 3 ps has been attributed to the (thermal or nonthermal) excitation of low-frequency modes that anharmonically couple to the amide-I modes.[22] Hence, the peptide backbone is still hot after 3 ps and contains a significant fraction of the large excess energy absorbed by the photoswitch. The T2D-IR spectrum recorded at 3 ps (Figure 3) is very similar to the stationary 2D-IR spectrum of the initial cis state, except for the sign (Figure 2b). This is in strong contrast to the schematic example described in Figure 1c. Despite the strong red-shifted absorption band in the T1D-IR spectrum, we do not observe

any distinct contribution from the transient photoproduct in the T2D-IR spectrum (expected at arrow 1 in Figure 3). If the transient photoproduct were to contribute to the T2D-IR spectrum to the same extent that it does in the T1D-IR spectrum, one would expect the T2D-IR spectrum look similar to Figure 1c (except for the overall sign because the shift is in the opposite direction).

After 20 ps, the stretching of the backbone conformation is almost finished, leaving the system in a highly nonequilibrium state.[22] The molecules have essentially cooled. The T1D-IR spectrum at $t_{UV} = 20$ ps shows a blue-shifted contribution from the transient photoproduct at $\omega_{pr} = 1685$ cm^{-1} (Figure 3, arrow 2). Again, hardly any signal is observed in the T2D-IR spectrum from the transient photoproduct (Figure 3, arrow 3). Furthermore, whereas the amplitude of the T1D-IR spectrum at 20 ps is 0.63 of the 3-ps signal, the ratio of the respective T2D-IR spectra is only 0.35.

The dynamics at delays larger than 20 ps is due to the peptide backbone adjusting to the stretched conformation.[22] After 200 ps, the T1D-IR spectrum has changed very little compared to that at 20 ps. In the T2D-IR spectrum, however, we now observe a negative (blue) band resulting from the transient photoproduct at $\omega_{pr} = 1685$ cm^{-1} (Figure 3, arrows 4 and 5). Furthermore, the negative (blue) band at $\omega_{pr} = 1635$ cm^{-1} is less elongated at 200 ps (Figure 3, arrow 6), and the positive (red) band in the center of the T2D-IR spectrum is oriented more vertically at longer delays (Figure 3, arrow 7).

After 1.7 ns, the negative band (blue) around $\omega_{pr} = 1685$ cm^{-1} is twisted toward the diagonal compared to the 200-ps spectrum (Figure 3, arrow 8). This effect is better seen in the cuts through the T2D-IR spectrum: at 1.7 ns, the minima of the signals at different pump frequencies are shifted apart (Figure 3, arrow 9). The T2D-IR spectrum after 1.7 ns looks very much like the schematic T2D-IR spectrum shown in Figure 1c.

V. Modeling of the Data

The most striking result of our T2D-IR experiment is the absence of an observable signal from the transient photoproduct at 3- and 20-ps delay times, although such a signal is clearly present in the T1D-IR spectra. To gain an understanding of this observation, we have to recall that a 2D-IR measurement can be viewed as a dynamic hole-burning experiment. As such, 2D-IR spectroscopy, in contrast to 1D spectroscopy, can distinguish between homogeneous and inhomogeneous broadening. For each pump frequency (i.e., for each horizonal cut through the 2D-IR spectra), we observe a hole with the *homogeneous* line width of the transition in resonance with the pump frequency (convoluted with the laser bandwidth) together with a red-shifted excited-state absorption (eq 1). However, because the anharmonic shift δ is roughly the same size as the homogeneous width, both signals partially cancel, and the amplitude of the measured signal decreases with increasing homogeneous width. The second key for understanding the outcome of the experiment is the small shift of the photoproduct absorption relative to that of the initial state (Figure 2a). As a result, the 2D-IR spectra of both species also strongly overlap and tend to cancel each other yet another time; the T2D-IR spectra are in fact *double*-difference spectra. Hence, a T2D-IR spectrum of the photoproduct with an enlarged homogeneous width, and hence a smaller overall amplitude, will be almost invisible in the double-difference spectrum, in which case the latter looks similar to the stationary 2D-IR spectrum of the initial state with interchanged sign.

To verify this working hypothesis, we used a very simple approach. We modeled the amide-I band as a single transition that is inhomogeneously broadened:

$$A_{inh}(\omega) = \int_{-\infty}^{\infty} G(\omega_0)\, A_{hom}(\omega - \omega_0)\, d\omega_0 \qquad (6)$$

The inhomogeneous distribution function $G(\omega_0)$ took into account both the presence of the (quasi-continuous) nine individual amide-I states as well as structural heterogeneity. We found that a Lorentzian distribution function $G(\omega_0)$ fits the linear absorption spectra better than a Gaussian distribution function. A total width of $\sim$38 cm^{-1} (fwhm) in both the cis and trans states and a 2-cm^{-1} blue shift upon cis $\rightarrow$ trans isomerization reproduced well the FTIR spectrum (Figure 2c). In agreement with the T1D-IR data, we used this blue shift for delays of 20 ps and longer. The shift of the central frequency after 3 ps can be estimated from the amplitude of the T1D-IR spectrum under the assumption that the depletion of the initial population is the same at 3 and 20 ps. It is set equal to -2 cm^{-1} (which represents a red shift). Using these parameters, model 1D difference spectra could readily be calculated (Figure 3). Because the frequency shifts are small compared to the total line width of the amide-I band, the negative signal from the initial state and the positive signal from the transient product state cancel strongly and the difference signal has the form of the first derivative of the absorption spectrum.

Two-dimensional IR spectra were calculated by weighing the 2D-IR response of a homogeneous line, calculated as in Figure 1 (eq 1), with the inhomogeneous distribution function $G(\omega_0)$:

$$\Delta A_{2D}(\omega_{pu}, \omega_{pr}) = \int_{-\infty}^{\infty} G(\omega_0)\, n_{ex}(\omega_{pu}, \omega_0) \times [A_{hom}(\omega_{pr} - \omega_0 + \delta) - A_{hom}(\omega_{pr} - \omega_0)]\, d\omega_0 \qquad (7)$$

Cross peaks between the various amide-I states were neglected in this approach. The homogeneous width could be deduced from the stationary 2D-IR spectrum (Figure 2d) and is $\gamma_i \approx 12$ cm^{-1}, in agreement with earlier results.[19] A typical value of 16 cm^{-1} was used for the anharmonicity δ.[3] To reproduce the time dependence of the T2D-IR spectra, we slightly varied the homogeneous broadening γ_t of the transient photoproduct as the only free parameter, keeping all other parameters constant. Although the T1D-IR difference spectra at 20 ps, 200 ps, and 1.7 ns are almost indistinguishable under these assumptions, the T2D-IR spectra depend sensitively on the homogeneous line width of the transient species. Good agreement with the experimental data was obtained with the homogeneous width of the photoproduct decreasing from $\gamma_t = 16$ cm^{-1} at 3 ps and $\gamma_t = 13.5$ cm^{-1} at 20 ps to $\gamma_t = 12.1$ cm^{-1} at 1.7 ns (Figure 3). The model T2D-IR spectrum would be symmetric for $\gamma_i = \gamma_t = 12$ cm^{-1} (as in Figure 1c), a situation that is almost reached after 1.7 ns. We verified that a variation of the homogeneous width γ_i and more detailed calculations that explicitly use the experimental T1D-IR spectra lead to very similar results.[25] In particular, an $\sim$10% change in γ_t between 20 ps and 1.7 ns is always required to reproduce the experimental results.

The simulated T2D-IR spectra can almost quantitatively explain all of the experimentally observed features, despite the crudeness of the model. In particular, the lack of an observable transient product band in the 3- and 20-ps T2D-IR spectra (Figure 3, arrow 1 and 3) and its appearance at $\omega_{pr} = 1685$ cm^{-1} at later times (Figure 3, arrow 4 and 5) are perfectly reproduced. Also, the more subtle changes (i.e., tilts and shifts of the various T2D-IR bands (Figure 3, arrows 6$-$9)) are well described. Note that a minor change in the homogeneous line

width of only 10% between 20 ps and 1.7 ns is sufficient to cause appreciable changes in the T2D-IR difference spectra. The reason for this high sensitivity is the small shift in the amide-I band upon cis−trans isomerization relative to its total line width (Figure 2a), leading to an almost complete cancellation of the various contributions in the T2D-IR spectra. Hence, even minor changes in the absolute 2D-IR spectra can lead to measurable effects in the T2D-IR spectrum. As a result of the difference measurement, the relative change in the homogeneous width γ_t can be measured much more accurately than its absolute value.

VI. Discussion

Spectral dephasing of a vibrational transition in the condensed phase is commonly related to stochastic fluctuations of its transition frequency.[26] In this approach, both linear and nonlinear spectroscopy are described in terms of the transition frequency fluctuation autocorrelation function $\langle \delta\omega(t)\, \delta\omega(0)\rangle$, where $\delta\omega(t)$ is the instantaneous deviation of the vibrator's frequency from its average value.[4,27,28] The vibrator is coupled to a fluctuating bath that may include inter- or intramolecular degrees of freedom. As the average transition frequency of the amide-I band is related to the average backbone structure,[15] fluctuations of the transition frequency reflect the dynamics of the backbone as well as of surrounding solvent molecules.

In this context, it is frequently found that the frequency fluctuation correlation function decays on (at least) two times scales:[29] (i) an ultrafast, inertial component on a 100-fs time scale and (ii) a slower, diffusion-controlled component on a time scale of many picoseconds. In the case of vibrational transitions, the ultrafast component is typically in the motional narrowing limit (i.e., its correlation time τ_c is faster than or of the same order of magnitude as the dephasing time $T_2^{-1} \equiv \langle \delta\omega(0)^2\rangle \tau_c$).[4,19,28] Hence, the homogeneous line width γ_t in our experiment is an exclusive measure of the fast (<1 ps) part of the total fluctuations of the system. The experimental data reveal that this fast contribution is more pronounced when the system is far from equilibrium. In the following text, we will discuss four possible explanations for this observation:

Temperature Effect. The UV photons of the pump pulse carry an energy of 3 eV (≙290 kJ/mol). We estimate an upper limit of 220 °C for the temperature of the molecule having absorbed an UV photon by Boltzmann distributing this energy over all normal modes. Normal modes have been calculated on the AM1 level for a geometry generated by an optimization of the trans state using the Gaussian 98 program package.[30] This estimate is considered to be an upper limit because a significant fraction of the energy is dissipated directly into the solvent during the first few picoseconds of the isomerization (an estimated factor of ∼0.5).[31] The temperature jump gives rise to a red shift of about -2 cm^{-1} in the 3-ps T1D spectrum as a result of the (thermal or nonthermal) excitation of anharmonically coupled low-frequency modes,[22] an effect that has been studied in detail in ref 32. The observed red shift of -2 cm^{-1} is in agreement with an estimate of ∼100 °C for the temperature jump.[33]

A temperature rise of that order of magnitude after 3 ps could certainly cause faster fluctuations of the molecule and hence the broader homogeneous line width that we observe. After 20 ps, however, the red-shifted band, which we may use as a built-in thermometer, has vanished, suggesting that the system has cooled to the bath temperature. Using the observed cooling rate of (4 ps)$^{-1}$,[22] we conclude that the temperature is elevated by less than 1 °C after 20 ps. The temperature dependence of vibrational dephasing in the protein environment has been investigated in detail and has revealed an Arrhenius law with an activation energy of ∼600 cm^{-1}.[34] If we use this scaling law, we find that a temperature rise of 10 °C would be required to explain the observed 10% broadening of the homogeneous line width after 20 ps. This discrepancy of 1 order of magnitude calls for alternative explanations.

Hole Burning in a Nonequilibrium Ensemble. The 2D-IR part of the experiment is performed on a nonequilibrium ensemble. Strictly speaking, the standard procedure to describe third-order nonlinear IR spectroscopy[4,27,28] should break down in this case. One could imagine that a hole burned into a distribution, which evolves in time (i.e., a nonequilibrium distribution), broadens in a different way than a hole burned into a stationary distribution. However, we have performed model calculations that show that this effect is too small to account for the additional 10% homogeneous broadening observed experimentally at 20 ps. Indeed, because of a clear separation of time scales, the 2D-IR experiment is actually performed on a quasi-equilibrium ensemble. A full account of this work will be given elsewhere.

Solvent Effect. A large contribution to the frequency fluctuation correlation function giving rise to dephasing and spectral diffusion originates from solvent fluctuations. This can be seen, for example, in the similar homogeneous dephasing rate of *N*-methylacetamide (NMA), which contains only a single peptide unit without the flexibility of the peptide backbone around the (ϕ, ψ) degrees of freedom.[19] The temperature argument given above applies in the same way to the solvent (i.e., a temperature jump on the order of 1 °C after 20 ps should be too small to account for the observed amount of broadening). In addition, the time scale on which the change of the homogeneous width takes place (an appreciable effect is still observable after 200 ps) is considerably longer than that for the solvation of DMSO, which contains a small (10%) 10-ps component.[35] Nevertheless, it is possible that the C═O groups are more exposed to the solvent during the early phase because of structural rearrangements and hence dephase faster. However, the homogeneous widths of the cis and trans ensembles in equilibrium are the same despite the very different structural distributions obtained from NMR analysis.[20] This can be deduced from the symmetric pattern of the late 1.7-ns T2D-IR spectrum (well reproduced in the simple model of Figure 1c), which turns out to be an extraordinarily sensitive measure of small differences in the homogeneous widths of reactant and transient photoproducts. Hence, it seems unlikely that the solvent alone is responsible for the observed effect between 20 ps and 1.7 ns.

Dimensionality of the Potential Energy Surface. A significant part of homogeneous dephasing can originate directly from fluctuations of the peptide backbone.[18] Hence, its change in time would reflect properties of the part of the potential energy surface that the molecules sample at a given UV pump−2D-IR probe delay time. The relevant time scale for homogeneous broadening (<1 ps) is too fast for the system to cross any significant barrier on the order of k_BT. For example, jumps over the barrier between the two preferred conformations of trialanine, the smallest possible peptide with one pair of (ϕ, ψ) dihedral angles, take tens of picoseconds to nanoseconds.[36,37] However, there may be regions in the potential energy surface far from equilibrium that are more shallow and on which the molecule can move almost freely and hence quickly. In fact, it has been shown with the help of time-dependent 2D-IR experiments in combination with molecular dynamic (MD) simulations for trialanine that the sampling of the conformational space of a peptide can be very fast (100 fs) when the system is

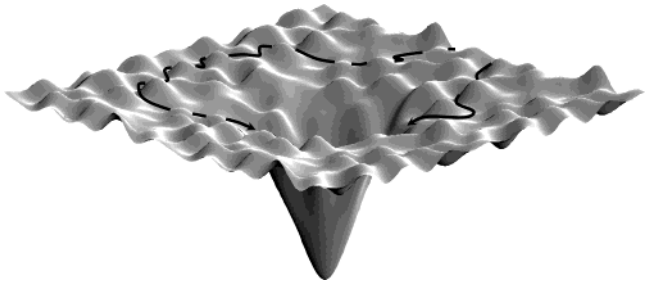

Figure 4. Schematic view of the random sampling on a rough potential energy surface.

located in a shallow part of the potential energy surface.[18] Along that line, the change in the homogeneous width with UV pump−2D-IR probe delay time would be an effect of the dimensionality of the accessible conformational space, which certainly becomes more confined when the backbone approaches its global energy minimum.

Figure 4 schematically depicts the system's search for its global minimum. Although the potential energy surface is rough, paths exist that do not have to *overcome* any barrier but may *pass by* barriers in a high-dimensional space. The potential energy surface is shallow along these directions so that the sampling of the surface can proceed extremely quickly on time scales faster than <1 ps. Nevertheless, owing to the large dimensionality of the problem, it may take a much longer time until the system actually finds the global minimum. Once it is trapped, however, the conformational space is confined, and the fast fluctuation amplitude is diminished accordingly.

VII. Conclusions

We introduced the technique of transient two-dimensional infrared spectroscopy (T2D-IR) and applied it to the ultrafast conformational transition of a photoswitchable cyclic peptide. Substantial changes in the T2D-IR spectra are found at times where the T1D-IR spectra show only little time dependence, illustrating the information boost provided by 2D-IR spectroscopy. In contrast to 1D spectroscopy, 2D-IR can distinguish between homogeneous and inhomogeneous broadening. Transient 2D-IR spectroscopy allows one to determine these quantities for a nonequilibrium ensemble evolving on an ultrafast time scale. Because the amide-I band reflects the instantaneous conformation of peptides and proteins, homogeneous and inhomogeneous broadening reveal details of the conformational distribution and its dynamics, which cannot be obtained otherwise. We find that the homogeneous contribution to the total width of the amide-I band decreases during the course of the conformational transition. This effect is tentatively attributed to the change in the rate with which the potential energy surface is sampled. However, to distinguish this effect conclusively, which would have important consequences in understanding rough energy landscapes, from more trivial explanations (such as solvent fluctuations), support from MD simulations is clearly needed.

In the present paper, the discussion of the T2D-IR spectrum is limited to the effects of homogeneous and inhomogeneous broadening because the amide-I spectrum of the investigated peptide is not resolved into individual subbands. For the case of spectrally resolved amide-I vibrators, it has been shown that additional structural information is contained in the cross peaks of 2D-IR spectra. We find a transient cross peak between the carboxyl group of the aspartic acid side chain at 1720 cm^{-1} and the amide-I band (Figure 3, arrow 10), which would allow a more site-specific discussion of the conformational transition of that side chain; this point will be addressed in future work. The possibility of observing transient cross peaks gives rise to the hope that combined with site-specific isotope labeling the present technique may provide detailed pictures of the 3D structure, or structural distribution, of the peptide as it approaches its new equilibrium state and may help to construct a molecular movie.

Acknowledgment. We thank Gerhard Stock and Wolfgang Zinth for illuminating discussions. This work has been supported by the Swiss Science Foundation (2100-067573.02/1) and by the SFB 533 (grant A8) of the Ludwig-Maximilians-Universitaet, Munich.

References and Notes

(1) Tanimura, Y.; Mukamel, S. *J. Chem. Phys.* **1993**, *99*, 9496−9511.
(2) Hybl, J. D.; Albrecht, A. W.; Faeder, S. M. G.; Jonas, D. M. *Chem. Phys. Lett.* **1998**, *297*, 307−313.
(3) Hamm, P.; Lim, M.; Hochstrasser, R. M. *J. Phys. Chem. B* **1998**, *102*, 6123−6138.
(4) Hamm, P.; Hochstrasser, R. M. In *Ultrafast Infrared and Raman Spectroscopy*; Fayer, M. D., Ed.; Marcel Dekker: New York, 2001; pp 273−347.
(5) Woutersen, S.; Hamm, P. *J. Phys.*: *Condens. Matter* **2002**, *14*, R1035−R1062.
(6) Zhao, W.; Wright, J. C. *Phys. Rev. Lett.* **2000**, *84*, 1411−1414.
(7) Scheurer, C.; Mukamel, S. *J. Chem. Phys.* **2001**, *115*, 4989−5004.
(8) Golonzka, O.; Khalil, M.; Demirdöven, N.; Tokmakoff, A. *Phys. Rev. Lett.* **2001**, *86*, 2154−2157.
(9) Merchant, K. A.; Thompson, D. E.; Fayer, M. D. *Phys. Rev. Lett.* **2001**, *86*, 3899−3902.
(10) Zanni, M. T.; Ge, N. H.; Kim, Y. S.; Hochstrasser, R. M. *Proc. Natl. Acad. Sci. U.S.A.* **2001**, *98*, 11265−11270.
(11) Zanni, M. T.; Gnanakaran, S.; Stenger, J.; Hochstrasser, R. M. *J. Phys. Chem. B* **2001**, *105*, 6520−6535.
(12) Hamm, P.; Lim, M.; DeGrado, W. F.; Hochstrasser, R. M. *Proc. Natl. Acad. Sci. U.S.A.* **1999**, *96*, 2036−2041.
(13) Woutersen, S.; Hamm, P. *J. Phys. Chem. B* **2000**, *104*, 11316−11320.
(14) Woutersen, S.; Hamm, P. *J. Chem. Phys.* **2001**, *114*, 2727−2737.
(15) Krimm, S.; Bandekar, J. *Adv. Protein Chem.* **1986**, *38*, 181−364.
(16) Torii, H.; Tasumi, M. *J. Raman Spectrosc.* **1998**, *29*, 81−86.
(17) Hamm, P.; Woutersen, S. *Bull. Chem. Soc. Jpn.* **2002**, *75*, 985−988.
(18) Woutersen, S.; Mu, Y.; Stock, G.; Hamm, P. *Proc. Natl. Acad. Sci. U.S.A.* **2001**, *98*, 11254−11258.
(19) Woutersen, S.; Pfister, R.; Hamm, P.; Mu, Y.; Kosov, D. S.; Stock, G. *J. Chem. Phys.* **2002**, *117*, 6833−6840.
(20) Renner, C.; Cramer, J.; Behrendt, R.; Moroder, L. *Biopolymers* **2000**, *54*, 501−514.
(21) Wachtveitl, J.; Spörlein, S.; Fonrobert, B.; Renner, C.; Behrendt, R.; Moroder, L.; Zinth, W. In *Recent Advances in Ultrafast Spectroscopy*, Proceedings of the XII UPS Conference; Califano, S., Foggi, P., Righini, R., Eds.; Leo S. Olschki: Firenze, 2003; pp 385−396.
(22) Bredenbeck, J.; Helbing, J.; Sieg, A.; Schrader, T.; Zinth, W.; Renner, C.; Behrendt, R.; Moroder, L.; Wachtveitl, J.; Hamm, P. *Proc. Natl. Acad. Sci. U.S.A.* **2003**, *100*, 6452−6457.
(23) Bredenbeck, J.; Hamm, P. *Rev. Sci. Instrum.* **2003**, *74*, 3188−3189.
(24) Hamm, P.; Kaindl, R. A.; Stenger, J. *Opt. Lett.* **2000**, *25*, 1798−1800.
(25) Note that in the case of equal homogeneous broadening for initial and transient species the T2D-IR spectrum is given by the convolution of the T1D-IR response with the 2D-IR signal of a homogeneous line. In contrast to our experimental findings, the T2D-IR spectra at 20 and 200 ps would then be almost identical to the spectrum at 1.7 ns. The signal at 3 ps cannot be reproduced at all under this assumption. Indeed, the T1D-IR signals exclude any variations in the relative intensities of the product bands, which could have provided an alternative explanation for the growth of the signal belonging to the product species in the T2D-IR spectra.
(26) Kubo, R.; Toda, M.; Hashitsume, N. *Statistical Physics II: Nonequilibrium Statistical Mechanics*; Springer: Berlin, 1985.
(27) Mukamel, S. *Principles of Nonlinear Optical Spectroscopy*; Oxford University Press: Oxford, U.K., 1995.
(28) Hamm, P.; Lim, M.; Hochstrasser, R. M. *Phys. Rev. Lett.* **1998**, *81*, 5326−5329.
(29) Fleming, G. R.; Cho, M. *Annu. Rev. Phys. Chem.* **1996**, *47*, 109−134.

(30) Frisch, M. J.; Trucks, G. W.; Schlegel, H. B.; Scuseria, G. E.; Robb, M. A.; Cheeseman, J. R.; Zakrzewski, V. G.; Montgomery, J. A., Jr.; Stratmann, R. E.; Burant, J. C.; Dapprich, S.; Millam, J. M.; Daniels, A. D.; Kudin, K. N.; Strain, M. C.; Farkas, O.; Tomasi, J.; Barone, V.; Cossi, M.; Cammi, R.; Mennucci, B.; Pomelli, C.; Adamo, C.; Clifford, S.; Ochterski, J.; Petersson, G. A.; Ayala, P. Y.; Cui, Q.; Morokuma, K.; Malick, D. K.; Rabuck, A. D.; Raghavachari, K.; Foresman, J. B.; Cioslowski, J.; Ortiz, J. V.; Stefanov, B. B.; Liu, G.; Liashenko, A.; Piskorz, P.; Komaromi, I.; Gomperts, R.; Martin, R. L.; Fox, D. J.; Keith, T.; Al-Laham, M. A.; Peng, C. Y.; Nanayakkara, A.; Gonzalez, C.; Challacombe, M.; Gill, P. M. W.; Johnson, B. G.; Chen, W.; Wong, M. W.; Andres, J. L.; Head-Gordon, M.; Replogle, E. S.; Pople, J. A. *Gaussian 98*, revision A.5; Gaussian, Inc.: Pittsburgh, PA, 1998.

(31) Spörlein, S.; Carstens, H.; Renner, H. S. C.; Behrendt, R.; Moroder, L.; Tavan, P.; Zinth, W.; Wachtveitl, J. *Proc. Natl. Acad. Sci. U.S.A.* **2002**, *99*, 7998−8002.

(32) Hamm, P.; Ohline, S. M.; Zinth, W. *J. Chem. Phys.* **1997**, *106*, 519−529.

(33) Hamm, P.; Zureck, M.; Röschinger, T.; Patzelt, H.; Oesterhelt, D.; Zinth, W. *Chem. Phys. Lett.* **1997**, *268*, 180−186.

(34) Rector, K. D.; Engholm, J. R.; Rella, C. W.; Hill, J. R.; Dlott, D. D.; Fayer, M. D. *J. Phys. Chem. A* **1999**, *103*, 2381−2387.

(35) Horng, M. L.; Gardecki, J. A.; Papazyan, A.; Maroncelli, M. *J. Phys. Chem.* **1995**, *99*, 17311−17337.

(36) Smith, P. E. *J. Chem. Phys.* **1999**, *111*, 5568−5579.

(37) Mu, Y.; Stock, G. *J. Phys. Chem. B* **2002**, *106*, 5294−5301.